European Congress on Computational Methods in Applied Sciences and Engineering
ECCOMAS 2000
Barcelona, 11-14 September 2000

FLOW AND DISPERSION AROUND BUILDINGS: AN APPLICATION WITH FEFLO

Fernando E. Camelli ⋆, and Rainald Löhner ⋆

⋆Institute for Computational Science and Informatics (CSI) George Mason University, M.S. 4C7, Fairfax, VA 22030, USA e-mail: fcamelli@gmu.edu, web page: http://www.science.gmu.edu/∼fcamelli

Key words: mass transport, atmospheric dispersion, pollution, FEFLO.

Abstract. *A series of simulations were performed in order to test the accuracy of FEFLO for problems of flow and dispersion around buildings. The major case was extracted from the Evaluation of Modelling Uncertainty (project EMU)[1]. The simulations were run in "black box" mode, i.e. no tuning of parameters was allowed. The results obtained were in very close agreement with the available wind-tunnel data for the case selected. The accuracy is comparable with other codes. The results show that an Euler run with proper profile yields a fairly accurate answer.*

1 INTRODUCTION

The study of pollutant dispersion is a primary topic for science today. In our industrialized society it is impossible to avoid completely pollution. Therefore it is important to fully understand the complex process of dispersion and transport of pollutants. This process is related to different scales in space and time. The problem can be classified in three scales: *urban-local, regional* and *mesoscale*. This classification is a crude one and it is presented here just to make clear that solving the problem has different challenges and difficulties [2].

The present study is focused on the urban-local scale. Such scale can include geometry of spatial extend of several buildings. The flow and dispersion around buildings has been investigated for many years, in particular in the field of wind engineering and pollution. Very detailed descriptions of the flow behavior around bluff bodies [3] were done during the 80's. The effort done in those years was based on experimental results. In many cases the description was completely qualitative, with mathematical relations between physical variables of the problem as average wind inflow, density (ρ), temperature, etc. and characteristic measurements of the object (length:L, width:W and height:H, roughness (z_0), etc.). The arrival of supercomputers brought the possibility to attack the problem from a completely different perspective, one that can complement the old experimental procedures. The first taken steps in that direction solving the governing equations for problems where involved reasonable 2-d approximations are possible, for example street canyons [4]. The long-term trend is to move to full 3-D simulations [5, 6]. There are many reasons why the efficient and accurate solution of 3-D problems is desirable:

a) Industrial accidents and the prediction of the dispersion of polluting substances;

b) Intentional release of toxic substances in populated areas (e.g. subway incident in Japan);

c) Establishment of policy rules based upon results of different simulations;

For this reason it was decided to test the accuracy of FEFLO, a general-purpose flow solver [7, 8], for cases in which there is a bluff object, an incoming flow and a continuous release and available experimental data. The cases covered by the EMU report [1] satisfied the requirements because of the good experimental data available.

A series of simulations were performed in order to test the accuracy of FEFLO for problems of flow and dispersion around buildings. The major case was extracted from the Evaluation of Modelling Uncertainty (project EMU)[1]. The simulations were run in "black box" mode, i.e. no tuning of parameters was allowed. The problem was solved with two different approaches. First, all viscous effects were ignored, i.e. the Euler equations were solved. Secondly, Navier-Stokes equations (Reynolds Averaged Navier-Stokes) with *Smagorinsky* turbulence model. The results obtained were in very close agreement with

the available wind-tunnel data for the case selected. The accuracy is comparable with other codes (e.g. STAR-CD [1]). The results show that an Euler run with proper profile (e.g. logarithmic profile) yields a fairly accurate answer in a reasonable amount of time.

2 SET UP STEPS

In order to simulate any problem, it is necessary to perform a series of steps in order to arrive at the final result that is the numerical data. The following is a brief summary of these steps:

• Geometry definition of the problem, known as pre-processing. For that part a CAD tool to input geometry and boundary conditions of the problem is used.

• Generation of a grid that covers the computational domain. The FRGEN3D code was used to obtain unstructured meshes using the advancing front methodology [9, 10, 11, 12]. In this way any complex geometry can be generated automatically. The input for this step is the CAD file produced in the previous step.

• Given a mesh, it is possible to go to the solver step. In order to solve the problem FEFLO code was used[8]. FEFLO can solve compressible or incompressible fluid problems, coupled to structures as well as transport equations. The output of this step is the numerical result.

• The last step is to analyse the data obtained by the solver, called post-processing. It can be hard and tediuos to get some conclusion from the huge amout of data produced. Zfem, a general visualization tool, is used to help in the analysis [13, 14, 15].

A sketch of the complete process is shown in figure 1.

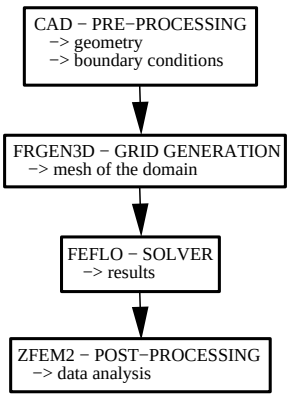

Figure 1: Steps for CFD run.

3 PROBLEM DISCRIPTION

The geometry in this case is an L-shape building placed in plane terrain as shown in figure 2.

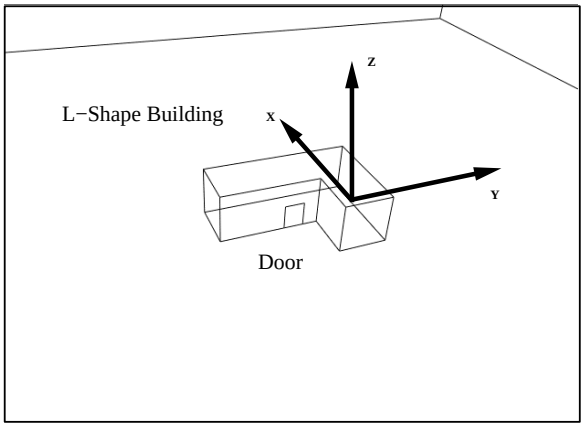

Figure 2: L-Shape Building Geometry.

The boundary conditions applied to this problem were fixed velocity and temperature in the inflow plane, characteristic in/outflow conditions in the outflow plane, the top plane of the computational domain and the lateral planes that are parallel to the direction of the incoming flow, and normal velocity equal to zero ($\vec{v}.\hat{n}|_{surface} = 0$) on the bottom surface and the surfaces of the building.

A non-uniform mesh was generated in order to have better flow field resolution in the areas of most interest, for example near the building. The mesh had 365,000 points and 2,030,000 tetrahedra. A surface mesh close to the building is shown in figure 3.

A flow parallel to the y-axis and with a velocity at building height: $U_h = 5m/s$ was imposed. A continuous release coming out from the door in the side of the building was prescribed. The area of the door is $20m^2$ and the release rate $Q_s = 20m^3/s$ in the normal door direction. The height of the building is $H = 10m$. Figure 3 shows a cross section from the top. The incoming wind was set to a logarithmic profile in the inflow plane:

$$U = \frac{u^*}{K} \ln\left(\frac{z}{z_0}\right) \tag{1}$$

where u^* is the friction velocity ($u^* = 0.0909U_h$), K is the von Karman constant ($K = 0.41$), and z_0 is the roughness length ($z_0 = 0.12m$) [1].

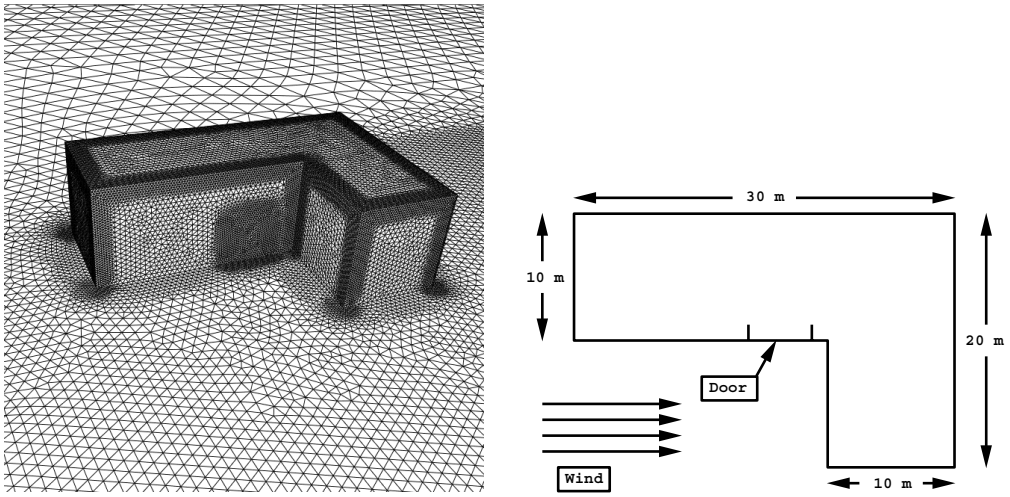

Figure 3: Left: L-Shape Building Mesh. Right: Top view of the L-Shape Building.

4 NUMERICS

The governing equations are given by the incompressible Navier-Stokes equations:

$$\nabla \mathbf{v} = 0 \tag{2}$$

$$\rho \frac{\partial \mathbf{v}}{\partial \mathbf{t}} + \rho \mathbf{v} \nabla \mathbf{v} + \nabla \mathbf{p} = \frac{1}{Re} \nabla \mu \nabla \mathbf{v} \tag{3}$$

$$\rho c_p \frac{\partial T}{\partial t} + \rho c_p \mathbf{v} \nabla \mathbf{T} = \frac{1}{RePr} \nabla k \nabla T \tag{4}$$

where c_p is the specific heat at constant pressure, ρ the density, Re is the Reynolds number and Pr is the Prandtl number:

$$Re = \frac{\rho_\infty |\mathbf{v}_\infty| \mathbf{L}}{\mu_\infty} \quad , \quad Pr = \frac{c_p \mu_\infty}{k_\infty} \tag{5}$$

where μ_∞ is the viscosity, k_∞ conductivity. The pressure p and velocities $\mathbf{v}$ are solved with a finite element projection method [16]. The concentration is solved in each time step using a finite element flux-corrected transport method (FEM-FCT) [8]. The equation for the concentration is:

$$\frac{\partial c}{\partial t} + \mathbf{v}.\nabla \mathbf{c} = \nabla \kappa \nabla c \tag{6}$$

where c is concentration, $\mathbf{v}$ is the flow field calculated at each time step and κ the diffusivity coefficient.

The problem was solved with two different approaches. First, all viscous effects were ignored, i.e. the Euler equations were solved. And secondly, Navier-Stokes equations (RANS) with Smagorinsky's turbulence model.

5 RESULTS

5.1 Flow Results

In this section qualitative results are presented for the flow field. All the plots were done with **zfem2** [13]. The first group of plots correspond to the Euler solution and second one to the RANS and Smagorinsky model.

5.1.1 Euler with Uniform Inflow:

Figure 4 depicts the velocity flow field for an uniform inflow using an Euler solver:

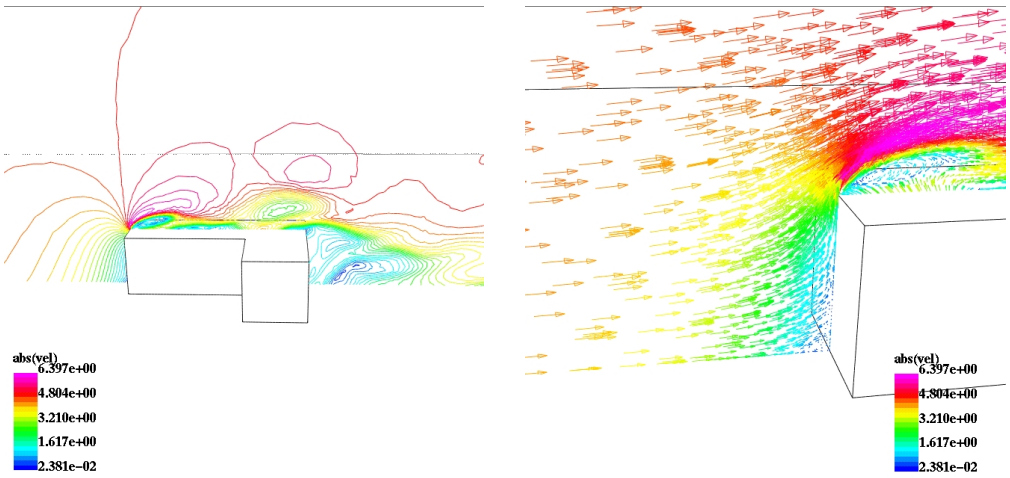

Figure 4: Euler Case with Uniform Flow. Left: Contour Lines for the Velocity. Right: Vector Plot for the Velocity.

Observe that no **horseshoe vortex** is present.

5.1.2 Euler Flow with Logarithmic Inflow:

Left figure 5 shows the contour lines of the absolute value of the velocity in a plane perpendicular to the x direction that is on the main flow direction. One can clearly see the separation due to the bluff corner of the building. The separation and reattachement follows the patterns discussed the literature [3].

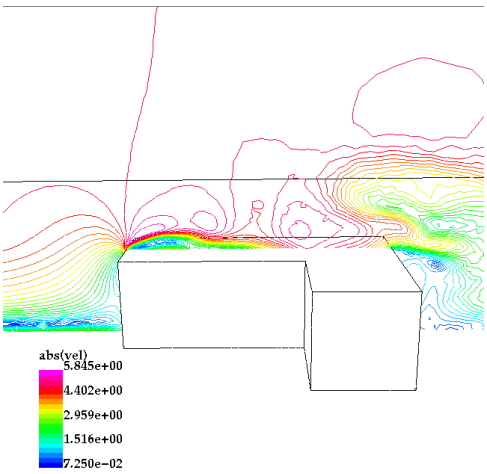

Figure 5: Euler Case with Log-Inflow. Contour Lines for the Velocity.

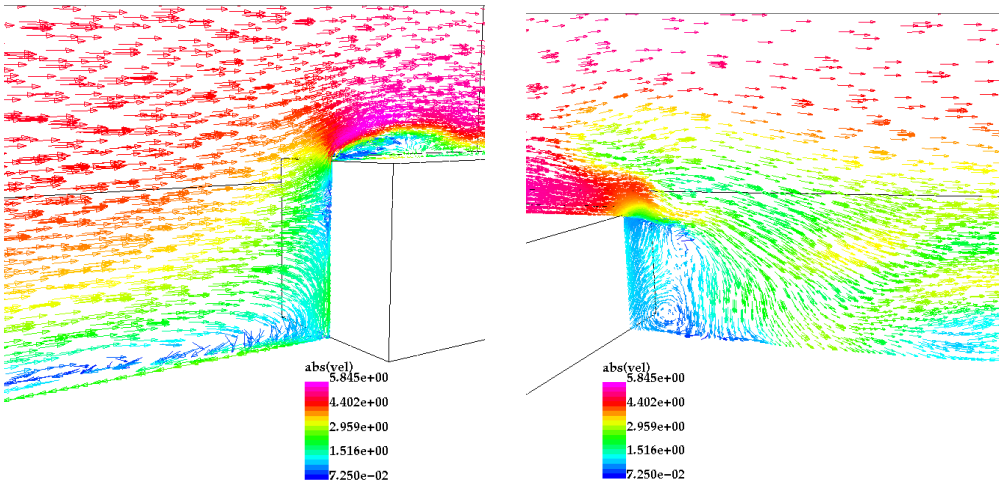

Figure 6: Euler Case with Log-Inflow. Vector Plot for the Velocity. Left: Upwind. Right: Downwind.

Left figure 6 shows the vector plot of the velocity and the recirculation at the upwind wall of the building. As Hosker [3] remarks, there is a big vortex in front of the obstacle related with the kind of boundary layer profile in the incoming wind. It must be emphasized that if the incoming flow is uniform, this recirculation does not exist. The down-wind face is shown in the right figure 6, and a big recirculation is visible. All these plots are from the Euler simulation and without any other assumption. It is possible to conclude from the results obtained that an Euler run and a proper boundary layer profile give qualitatively good results.

5.1.3 Turbulent Flow (Smagorinsky) with Logarithmic Inflow:

The results with the Smagorinsky model are showing more or less the same trends as Euler. The contour plot of the velocity in the figure 7 depicts the recirculation in the upwind and downwind parts of the building as the separation on the roof with the reattachement.

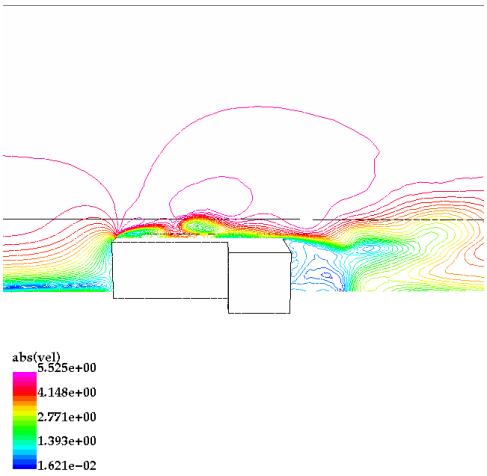

Figure 7: Smagorinsky Case Contour Lines for the Velocity.

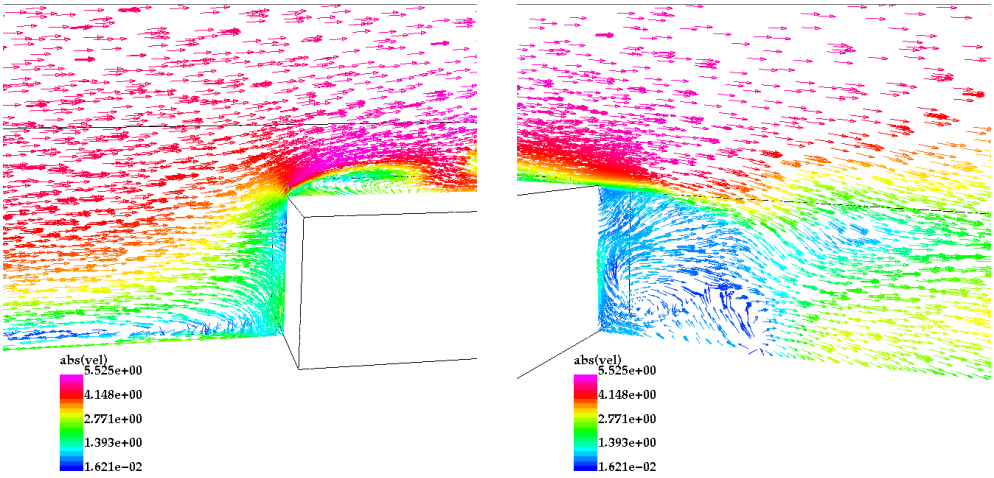

Figure 8: Smagorinsky Case Vector Plot for the Velocity. Left: Upwind. Right: Downwind.

Figure 8 shows the vector plot of velocity in the front and in the back of the building.

5.1.4 Isosurface of Concentration:

The isosurface of concentration at 10% for both cases, Euler and Smagorinsky, is showed at figures 9 and 10. Figure 9 shows a cloud not so diffusely because of the fact that it is an Euler run, but in figure 10 the cloud is more diffused in the back and at both sides of the building. The color scale on top of both clouds is the velocity at those points.

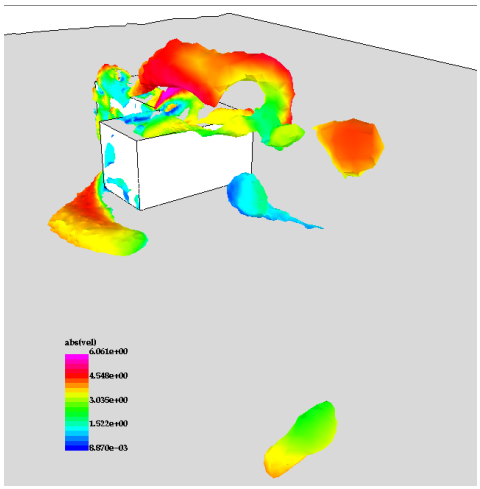

Figure 9: Euler Case 10% isosurface of concentration.

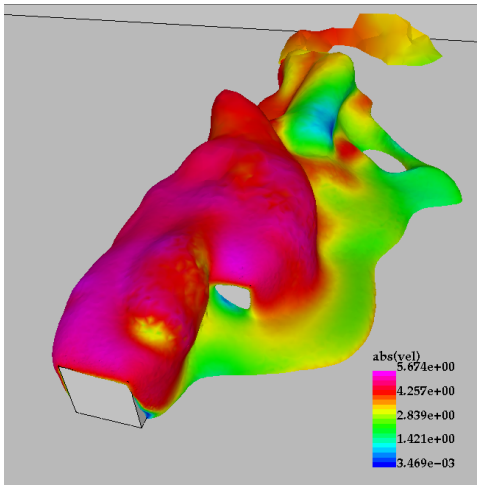

Figure 10: Smagorinsky Case 10% isosurface of concentration.

5.2 Horseshoe vortex

The logarithmic profile inflow produces a characteristic upwind close to the building, and one can observe that particular flow for different heights of uncoming wind with ribbons that are colored with the wind velocity. In the figures 11 12 13 and 14 it is observed the *horseshoe vortex* well described in the Hosker review of 1980 [3].

5.2.1 Euler with Logarithmic Inflow:

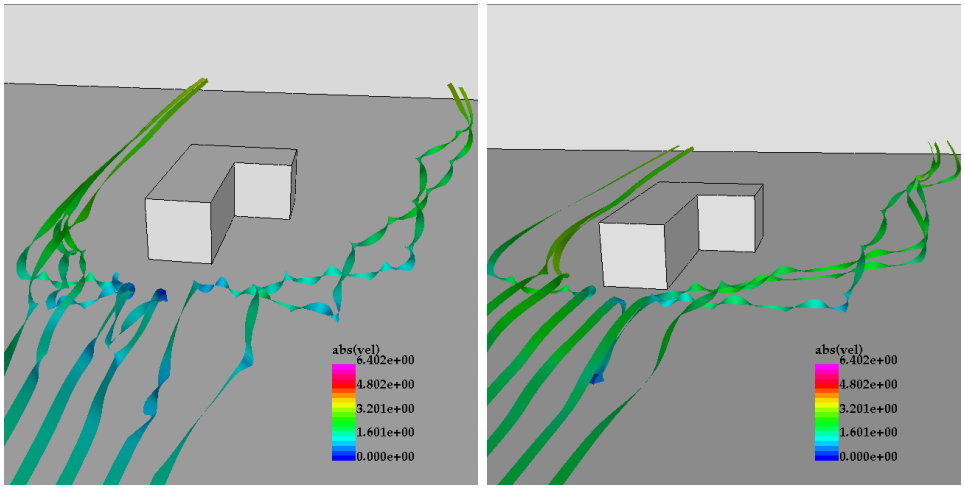

Figure 11: Euler: Ribbons of Velocity. Left: 0.2 m from the floor. Right: 1.0 m from the floor.

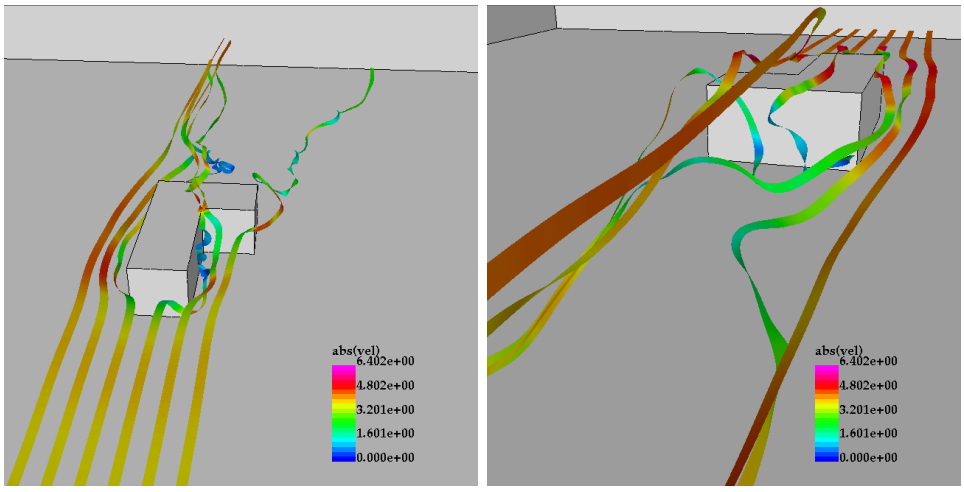

Figure 12: Euler: Ribbons of Velocity. Left: 5.0 m from the floor. Right: 8.0 m from the floor.

5.2.2 Smagorinsky with Logarithmic Inflow:

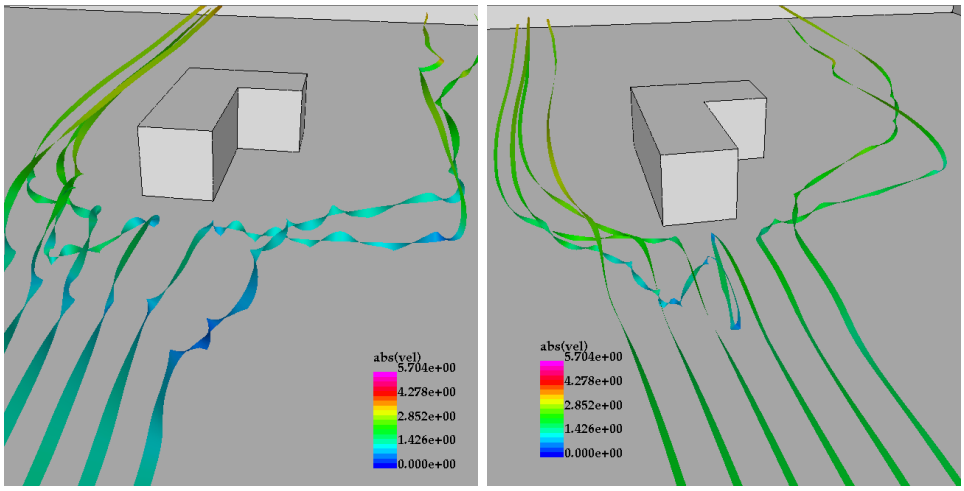

Figure 13: Smagorinsky: Ribbons of Velocity. Left: 0.2 m from the floor. Right: 1.0 m from the floor.

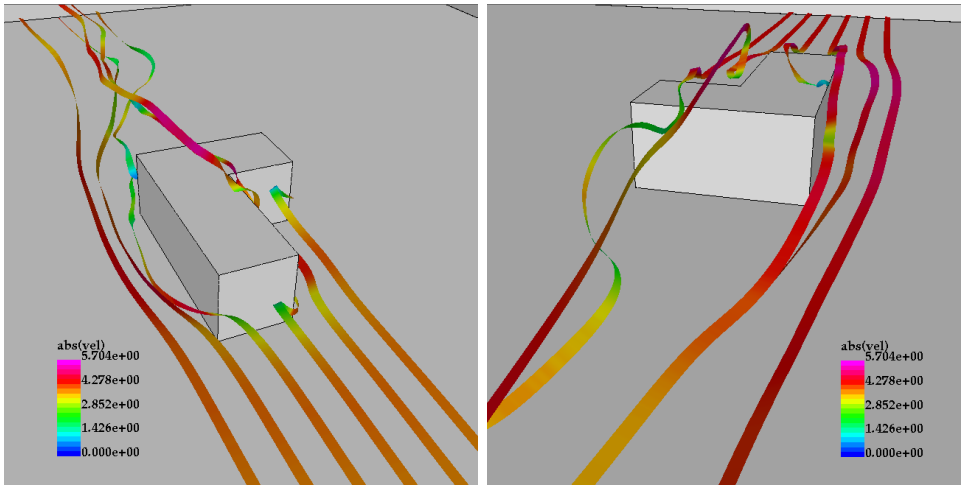

Figure 14: Smagorinsky: Ribbons of Velocity. Left: 5.0 m from the floor. Right: 8.0 m from the floor.

5.3 Comparison with The Wind Tunnel Results

The numerical results were compared against the data obtained from the wind-tunnel experiment done for the people of EMU project [1]. The concentration is expressed as a non-dimensionaled value called C^*:

$$C^* = \frac{cU_h H^2}{Q} \tag{7}$$

where c is concentration, U_h is the average velocity at the height of the building roof, H is the height of the building ($10m$) and Q is the source emission rate ($Q = 20m^3/s$).

The mean concentration for different stations can be seen in figures 15 to 18.

5.3.1 Euler Dispersion:

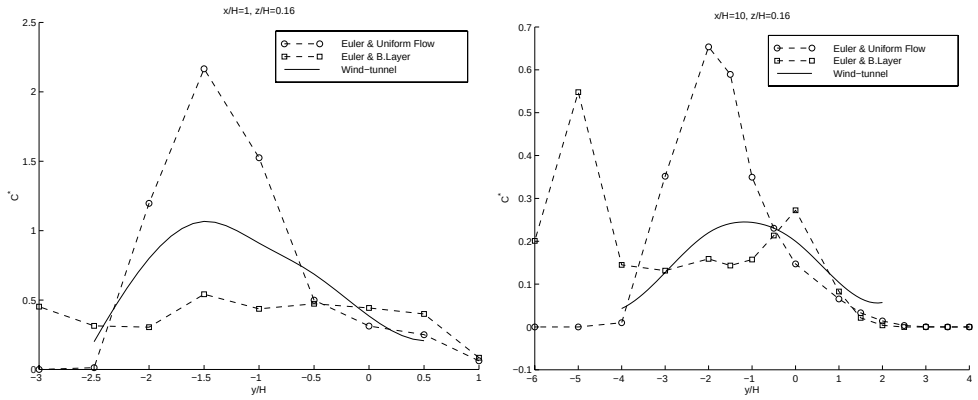

Figure 15: Euler Case Normalized Concentration.

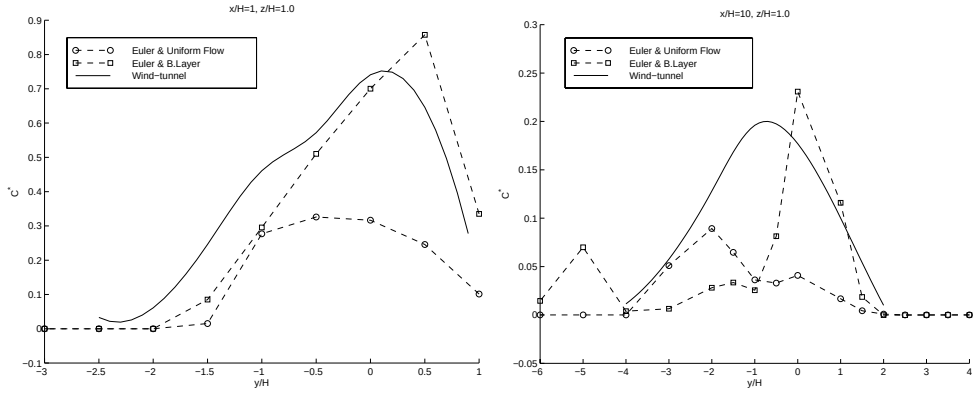

Figure 16: Euler Case Normalized Concentration.

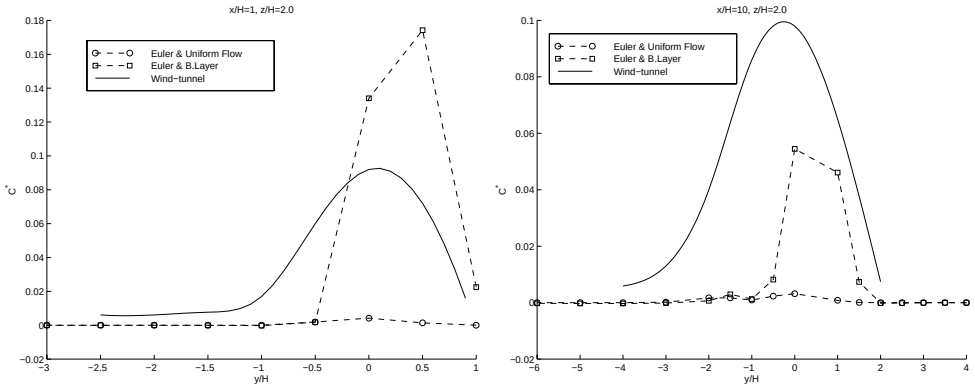

Figure 17: Euler Case Normalized Concentration.

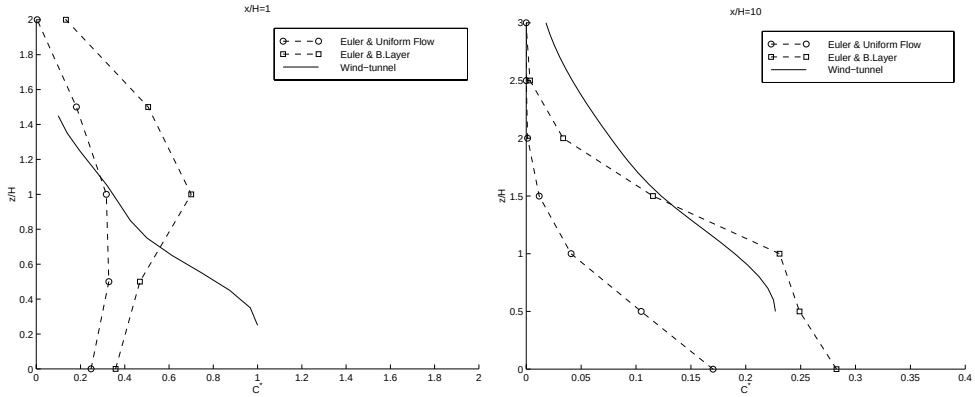

Figure 18: Euler Case Normalized Concentration.

5.3.2 Smagorinsky Dispersion:

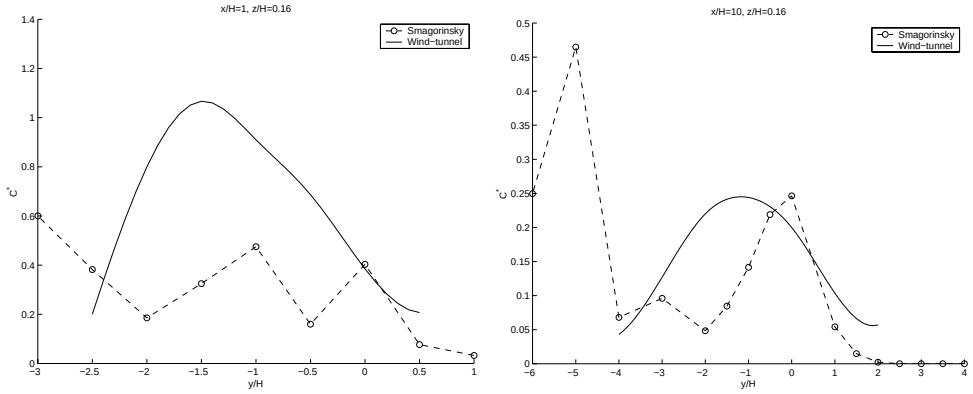

Figure 19: Smagorinsky Case Normalized Concentration.

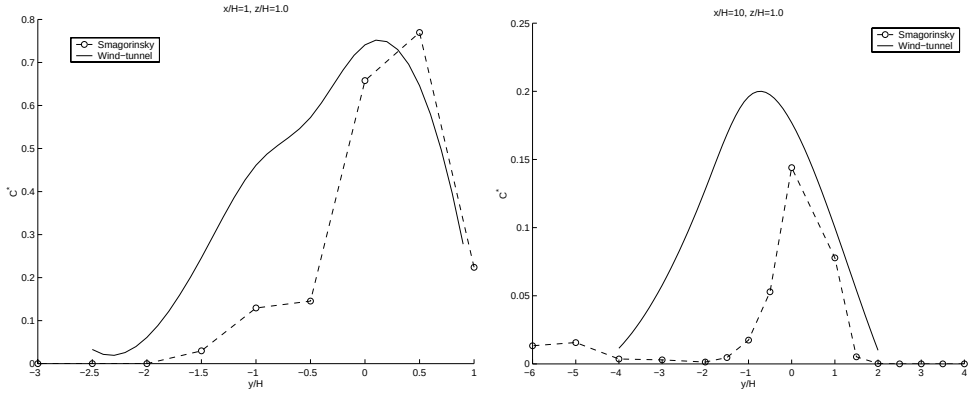

Figure 20: Smagorinsky Case Normalized Concentration.

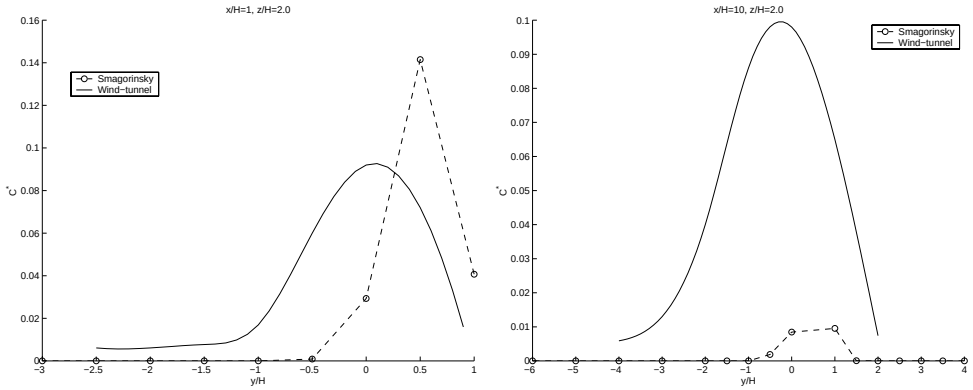

Figure 21: Smagorinsky Case Normalized Concentration.

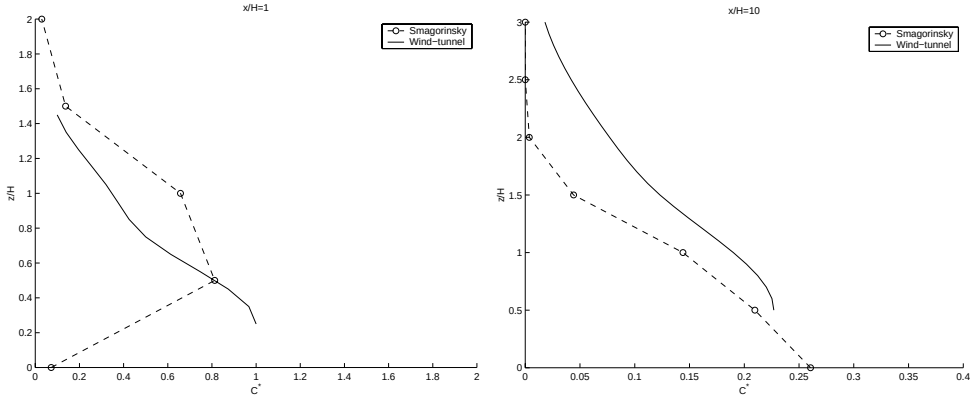

Figure 22: Smagorinsky Case Normalized Concentration.

6 CONCLUSIONS AND OUTLOOK

The study of problems of an small scale like a city or a group of buildings is still a very difficult topic [17]. In the context of the experimental research done along the years in that field and the utilization of the CFD techniques both together can be a very powerful combination to get important results. The small test done using FEFLO was successful in terms that code was used as a black box to solve the problem and the results are in agreement with the experimental data available. However, there are many points where it is necessary continuous working to get better results in the future. Since results with Euler and turbulent model are pretty similar that suggests that in this case of problems the geometry an the inflow wind drive the results for the macro scale. It was noticed that the kind of boundary layer profile in the incoming flow has a very strong influence on the results. Aspects such temperature and bouyancy should be included in next steps to have

a complete idea of the problem. Other points to emphasize are the possibilities to see all the features mention by Hosker [3] in the flow profile on the upwind and downwind face of the building.

REFERENCES

References

[1] *Evaluation of Modelling Uncertainty, CFD Modelling 0f Near-Field Atmospheric Dispersion*. Project EMU final report (1997).

[2] S. Pal Arya, *Air Pollution Meteorology and Dispersion*, Oxford University Press (1999).

[3] R.P. Hosker, "Flow and Diffusion Near Obstacles", in: D.Raderson (Ed.), *Atmospheric Science and Power Production. US Dept of Energy*, DOE/CR-2521 (US Nuclear Regulatory Commission) (1980).

[4] J.F. Sini, S. Anquetin, and P.G. Mestayer, "Pollutant Dispersion and Thermal Effects in Urban street Canyons", *Atmospheric Environment* **30**, No. 15, pp. 2659-2677 (1995).

[5] I.R. Cowan, I.P. Castro, and A.G. Robins, "Numerical Considerations for Simulations of Flow and Dispersion around Buildings", *J. Wind Eng. Ind. Aerodyn.* **67-68**, pp. 535-545 (1997).

[6] P.Dawson, D.E. Stock, and B.Lamb, "The Numerical Simulation of Airflow and Dispersion in Three-Dimensional Atmospheric Recirculation Zones", *J. Appl. Meteor.* **30**, pp. 1005-1024 (1991).

[7] R. Ramamurti and R. Löhner, "A Parallel Implicit Incompressible Flow Solver Using Unstructured Meshes", *Computers and Fluids* **5**, pp. 119-132 (1996).

[8] R. Löhner, K. Morgan, J. Peraire, and M. Vahdati, "Finite Element Flux-Corrected Transport (FEM-FCT) for Euler and Navier-Stokes Equations", *Int. J. Num. Meth. Fluids* **7**, pp. 1093-1109 (1987).

[9] R. Löhner, "Recent Progress in Tetrahedral Grid Generation via the Advancing Front Technique", *3rd. International Meshing Roundtable*, Albuquerque, NM, October 1994.

[10] R. Löhner, "Extending the Range of Applicabilty and Automation of the Advancing Front Grid Generation Technique", *AIAA* 96-0033 (1996).

[11] R. Löhner, "Automatic Unstructured Grid Generators", *Finite Elements in Analysis and Design* **25**, pp. 111-134 (1997).

[12] R. Löhner, "Generation of Unstructured Grids Suitable for RANS Calculations", *AIAA* 99-0662 (1999).

[13] J.R. Cebral, "ZFEM: Collaborative Visualization for Parallel Multidisciplinary Applications", *Proceedings of Parallel CFD'97*, Manchester, U.K., May 19-21 (1997).

[14] J.R. Cebral, and R. Löhner, "Interactive On-Line Visualization and Collaboration for Parallel Unstructured Multidisciplinary Applications", *AIAA* 98-0077 (1998).

[15] J.R. Cebral, and R. Löhner, "Advances in Visualization: Distribution and Collaboration", *AIAA* 99-0693 (1999).

[16] R.Ramamurti, and R. Löhner, "A Parallel Implicit Incompressible Flow Solver Using Unstructured Meshes", *Computers and Fluids* **5**, pp. 119-132 (1996).

[17] P.G. Mestayer, S. Anquetin, "Climatology of Cities", in: A.Gyr,F.Rys (Ed.), *Diffusion and Transport of Pollutants in Atmospheric Mesoscale Flow Fileds*, pp. 165-189 (1995).